J Mol Model (2013) 19:2715–2722
DOI 10.1007/s00894-012-1520-2

ORIGINAL PAPER

Explaining reaction mechanisms using the dual descriptor: a complementary tool to the molecular electrostatic potential

Jorge Ignacio Martínez-Araya

Received: 29 March 2012 / Accepted: 25 June 2012 / Published online: 31 July 2012

Abstract The intrinsic reactivity of cyanide when interacting with a silver cation was rationalized using the dual descriptor (DD) as a complement to the molecular electrostatic potential (MEP) in order to predict interactions at the local level. It was found that DD accurately explains covalent interactions that cannot be explained by MEP, which focuses on essentially ionic interactions. This allowed the rationalization of the reaction mechanism that yields silver cyanide in the gas phase. Other similar reaction mechanisms involving a silver cation interacting with water, ammonia, and thiosulfate were also explained by the combination of MEP and DD. This analysis provides another example of the usefulness of DD as a tool for gaining a deeper understanding of any reaction mechanism that is mainly governed by covalent interactions.

Keywords Cyanide anion · Water · Ammonia · Thiosulfate anion · Silver complexes · Ligand · Complexation agent · Local reactivity · Dual descriptor · Silver exploitation · Conceptual DFT

Introduction

The molecular electrostatic potential [1, 2] allows us to quantify ionic interactions between two species. When written in terms of atomic units, it takes the form

$$V(\mathbf{r}) = \sum_{A} \frac{Z_A}{|\mathbf{R}_A - \mathbf{r}|} - \int \frac{\rho(\mathbf{r}')}{|\mathbf{r}' - \mathbf{r}|} d\mathbf{r}', \quad (1)$$

J. I. Martínez-Araya (✉)
Vicerrectoría de Investigación y Desarrollo and Facultad de Ingeniería, Campus República, Sede Santiago,
Universidad Pedro de Valdivia,
Av. Libertador Bernardo O'Higgins 2222,
8370962 Santiago, Chile
e-mail: jorge.martinez.doc@upv.cl

J. I. Martínez-Araya
e-mail: jmartiar@gmail.com

where Z_A is the atomic number of nucleus A, $\mathbf{R}_A$ is the position of nucleus A, and $|\mathbf{r}'-\mathbf{r}|$ is its distance from point $\mathbf{r}$.

On the other hand, within the framework of conceptual DFT [3–5, 6], when covalent interactions are more relevant than electrostatic interactions, Morell et al. [7–13] proposed that a local reactivity descriptor (LRD) called the dual descriptor (DD) $f^{(2)}(\mathbf{r}) \equiv \Delta f(\mathbf{r})$ should be used as a measure of the local reactivity. Although the DD was derived several years ago, a solid physical interpretation of it was not available at that time [14]. They originally used the notation $\Delta f(\mathbf{r})$ for the DD, but this has since been replaced by the modern notation $f^{(2)}(\mathbf{r})$ in order to highlight the fact that this is a second-order Fukui function. Physically speaking, it indicates the nucleophilic and electrophilic sites in a molecular system. Mathematically, it is defined in terms of the derivative of the Fukui function, $f(\mathbf{r})$ [5], with respect to the number of electrons, N. Using a Maxwell relation, this LRD can be interpreted as the variation in η (the molecular hardness, which measures the resistance to charge transfer [15]) with respect to $\upsilon(\mathbf{r})$, the external potential. $f^{(2)}(\mathbf{r})$ (as described by Morell et al. [7, 8]) is defined as follows:

$$f^{(2)}(\mathbf{r}) = \left(\frac{\partial f(\mathbf{r})}{\partial N}\right)_{\upsilon(\mathbf{r})} = \left[\frac{\delta \eta}{\delta \upsilon(\mathbf{r})}\right]_N. \quad (2)$$

As mentioned above, the DD allows us to simultaneously determine which of the sites in a system at point $\mathbf{r}$ are most likely to suffer nucleophilic attacks [$f^{(2)}(\mathbf{r})>0$] or electrophilic attacks [$f^{(2)}(\mathbf{r})<0$]. The DD has been shown to be a robust tool for predicting sites that are particularly vulnerable to nucleophilic or electrophilic attack; indeed, it is a much more efficient tool for achieving this aim than the Fukui function by itself, because the dual descriptor is able to discriminate sites that show true nucleophilic and electrophilic behavior. Therefore, some works have been published that demonstrate the power of $f^{(2)}(\mathbf{r})$ and all of the LRDs that depend on DD [10–12].

The general working equation that is used to calculate the DD is essentially the difference between the nucleophilic and electrophilic Fukui functions [7]. Calculating this to the first level of approximation implies the use of the finite difference method, where double the total electronic density of the original system is subtracted from the sum of the electronic density of the system with one more electron and the electronic density of the system with one less electron. Since calculating to this level of approximation is a computationally expensive task, a second level of approximation has been used for some years. This level of approximation includes the densities of the FMOs (making it much easier to compute the working equation):

$$f^{(2)}(\mathbf{r}) \simeq \rho_{\mathrm{L}}(\mathbf{r}) - \rho_{\mathrm{H}}(\mathbf{r}),$$

where the densities of the LUMO and HOMO are represented by $\rho_{\mathrm{L}}(\mathbf{r})$ and $\rho_{\mathrm{H}}(\mathbf{r})$, respectively. Molecular symmetry can influence the local reactivity, but it has also been demonstrated that the Fukui function must conserve the symmetry [16]. In addition, as the degeneration that may arise in frontier molecular orbitals is related to the molecular symmetry, this phenomenon has been taken into account within the framework of the second level of approximation by Martínez [17], who provided the following expression for closed-shell molecular systems:

$$f^{(2)}(\mathbf{r}) \simeq \frac{1}{p}\sum_{k=1}^{p}\rho_{\mathrm{L}\,k}(\mathbf{r}) - \frac{1}{q}\sum_{k=1}^{q}\rho_{\mathrm{H}\,k}(\mathbf{r}). \tag{3}$$

where

$$p\begin{cases} = 1 \Rightarrow & \mathrm{L1} \equiv \mathrm{LUMO} \\ > 1 \Rightarrow & \mathrm{L1} \equiv \mathrm{LUMO} \\ & \mathrm{L2} \equiv \mathrm{LUMO}+1 \\ & \mathrm{L3} \equiv \mathrm{LUMO}+2 \\ & \cdots\cdots\cdots\cdots \\ & \mathrm{L}p \equiv \mathrm{LUMO}+(p-1) \end{cases} ; q\begin{cases} = 1 \Rightarrow & \mathrm{H1} \equiv \mathrm{HOMO} \\ > 1 \Rightarrow & \mathrm{H1} \equiv \mathrm{HOMO} \\ & \mathrm{H2} \equiv \mathrm{HOMO}-1 \\ & \mathrm{H3} \equiv \mathrm{HOMO}-2 \\ & \cdots\cdots\cdots\cdots \\ & \mathrm{H}q \equiv \mathrm{HOMO}-(q-1) \end{cases}$$

This approximation has been applied, for example, to the local reactivity of Buckminsterfullerenes [18], in which case the DD was derived according to the symmetry of these molecules. A working equation for open–shell systems has also been suggested, but it was not used in the present work because all of the systems considered here are closed–shell systems.

Hence, when an interaction between two species is well described by using this LRD, it is said that the reaction is controlled by frontier molecular orbitals (or frontier-controlled), under the assumption that remaining molecular orbitals do not participate in the reaction.

The aim of the work described in this paper was to show how the dual descriptor, through the working equation (3), is a useful tool that can be utilized as a complement to the molecular electrostatic potential, thus providing more accurate insight into the interactions that occur among molecules during a particular reaction mechanism.

Computational methods

Cyanide anion, water, ammonia, and thiosulfate anion, along with their respective silver complexes, were geometrically optimized without symmetry restrictions according to the Schlegel algorithm [19] at the DFT level of theory. The functionals used in these calculations were the Becke three-parameter functional for exchange and the Lee–Yang–Parr functional for correlation [20–23]. The double-zeta quality LANL2DZ [24, 25] basis set was used to describe all atoms. Frequency calculations were performed at the same level of theory in order to ensure that each optimized structure corresponded to an energy minimum. 3D maps of the MEP and DD were generated. All calculations were carried out using the Gaussian 09 [26] code.

Discussion

A detailed analysis of the reaction mechanism to form silver cyanide

The global reaction

$$\mathrm{Ag^{+}} + 2\,\mathrm{CN^{-}} \rightarrow \left[\mathrm{Ag\,(CN)_2}\right]^{-}$$

can be decomposed into two elementary steps, thus giving the following reaction mechanism:

1) $\mathrm{Ag^{+}} + \mathrm{CN^{-}} \rightarrow \mathrm{AgCN}$
2) $\mathrm{AgCN} + \mathrm{CN^{-}} \rightarrow \left[\mathrm{Ag\,(CN)_2}\right]^{-}$

The ball-and-stick model depicted in Fig. 1 shows the connections and disconnections that occur among the atoms during this chemical reaction. The chemical bond is preferentially formed between the silver cation and the carbon atom from cyanide, according to the hard/soft acid/base principle established by Pearson [27–31], in such a way that the silver cation is considered to be a soft acid (electrophile) and the cyanide anion a soft base (nucleophile), through its carbon atom. The global interaction is well described by the MEP, as depicted in Fig. 2. However, it is important to note that, although MEP explains long-range interactions correctly, short-range interactions are better explained by DD, because this LRD is associated with site selectivity. In this work, we used DD for short–range interactions when MEP did not allow a specific atom to be selected in order to achieve the final product and/or a reaction intermediate.

Since DD has been shown to be a suitable tool for revealing the zones in molecules where covalent interactions should predominate over electrostatic interactions, studying this reaction mechanism represents a good way of demonstrating this capability of DD.

The reaction was divided into two elementary steps: (1) and (2) (see Fig. 1). The first elementary step is a typical electrostatic interaction where the silver cation reacts with the cyanide anion to form an uncharged silver complex. Negative and positive zones, color coded according to the predominance of electrons or nuclei, respectively, are shown in Fig. 2. Note that this typical electrostatic interaction can also be explained using the dual descriptor, because the positive phase of the dual descriptor for the silver cation will favorably interact with the negative phase for the cyanide anion, as indicated by Fig. 3. This electrically neutral silver complex, AgCN, then reacts with a second cyanide anion, CN^- to form the well-known silver complex $[Ag(CN)_2]^-$. However, the molecular electrostatic potential, on its own, is not able to explain why the cyanide anion reacts preferentially through its carbon atom, not through the nitrogen atom. This is a clear signal that the chemical bond involved in the formation

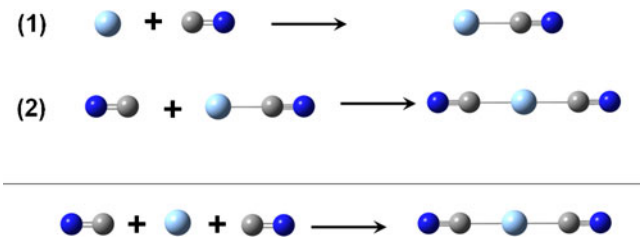

Fig. 1 Ball-and-stick model of the reaction mechanism leading to the formation of the $[Ag(CN)_2]^-$ silver complex. Atoms are color coded as follows: *blue* nitrogen, *gray* carbon, *light blue* silver

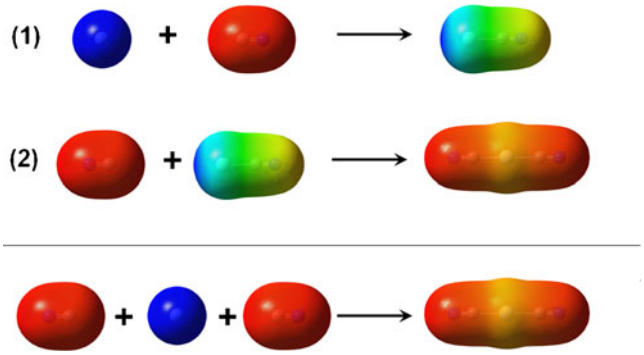

Fig. 2 The reaction mechanism leading to the formation of the silver complex, shown in terms of 3D maps of the molecular electrostatic potential (MEP), $V(\mathbf{r})$. MEP values vary from negative (*red*) to positive (*blue*); *red-colored zones* indicate sites where the effects of electrons are dominant (electrically negative), *green-colored zones* indicate sites where the effects of nuclei and electrons are balanced, while *blue-colored zones* show sites where the effects of nuclei are dominant (electrically positive). The interval $\{V(\mathbf{r})\}_{min} \leq V(\mathbf{r}) \leq \{V(\mathbf{r})\}_{max}$ is therefore shown. Isosurfaces of 0.001 a.u. are depicted

of these silver complexes possesses a markedly covalent nature. In other words, there is a subtle distinction between C and N in CN^- that prompts us to use DD, because in this case we expect that covalent interactions drive the reaction, which would explain why the carbon atom of cyanide prefers to form a bond with the silver atom of AgCN.

This reaction mechanism can then be rationalized in terms of the dual descriptor (adapted to the molecule's symmetry). The silver cation and cyanide anion are classified as closed-shell systems. The silver cation has a singly degenerate HOMO and fivefold-degenerate LUMO, thus implying $q=1$ and $p=5$; the cyanide anion has a doubly degenerate HOMO and a singly degenerate LUMO, so $q=2$

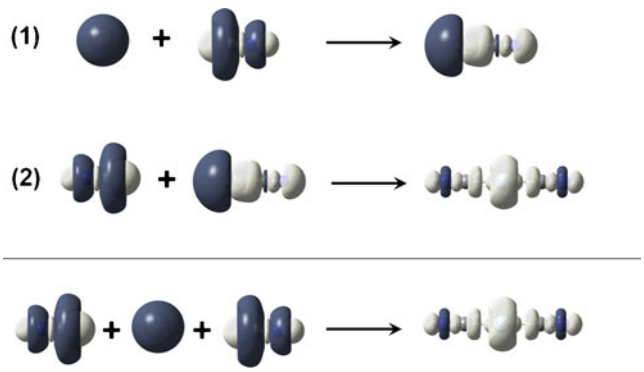

Fig. 3 The reaction mechanism leading to the formation of the silver complex, shown in terms of 3D maps of the dual descriptor (DD), $f^{(2)}(\mathbf{r})$. A *dark-colored lobe* implies that $f^{(2)}(\mathbf{r})>0$, thus indicating that nucleophilic attacks will preferentially occur there; a *light-colored lobe* implies that $f^{(2)}(\mathbf{r})<0$, thus indicating that electrophilic attacks will preferentially occur there. Isosurfaces of 0.001 a.u. are depicted

and $p=1$. The dual descriptors obtained for each species after applying Eq. 3 are depicted in Fig. 3.

The DD of the cyanide anion exhibits nucleophilic lobes that are localized on carbon and nitrogen (light-colored lobes, Fig. 3), while its electrophilic region occurs around the chemical bond established between these two atoms (dark-colored lobe, Fig. 3). In the case of the silver cation, the dual descriptor shows that there is an electrophilic lobe in an outer shell, whereas the nucleophilic lobe is localized inside the electrophilic lobe. This apparent anomaly may be due to the cationic nature of the silver cation; it indicates that the silver cation generally does not want to donate electrons. Hence, in the case of the silver cation, we do not need to use the dual descriptor to reach such a conclusion; the molecular electrostatic potential will reveal this behavior. This is based on the fact that the silver cation is a soft Lewis acid—it can only receive electrons, not donate them.

More interesting is the case of the cyanide anion. In specific interactions with cyanide, the DD occurs around the silver cation as shown in Fig. 3. Since cyanide is a diatomic heterogeneous species, the nucleophilic and electrophilic lobes are bigger on carbon than on nitrogen, so the most favorable interaction with a electrophile is going to occur through the carbon atom, not through the nitrogen atom.

The first elementary step leads to the formation of an electrically neutral silver complex, AgCN. Figure 2 reveals the negative and positive zones of this silver complex based on the molecular electrostatic potential. Using this figure, it is easy to predict that a favorable interaction with this complex will occur through its electrically positive region (which surrounds the Ag) when an electrically negative molecule or atom approaches AgCN. However, if this electrically negative species is a second CN^-, there will again be two possible sites at which a chemical bond could form: through the carbon atom or through the nitrogen atom of cyanide.

MEP cannot provide this level of information, but DD can. If we consider the DD for the second step (see Fig. 3), we can see how well the second cyanide interacts with AgCN. On an electrostatic basis, MEP reveals that the second cyanide approaches the silver atom of AgCN. From a covalent perspective, DD indicates that a favorable chemical bond forms between the silver atom from AgCN and the carbon atom, not the nitrogen atom, of this second cyanide.

A brief analysis of reaction mechanisms leading to the formation of other similar silver complexes

A similar analysis can be performed to explain some typical reaction mechanisms involving a silver cation that result in the formation of a silver complex. For each reaction we consider below, the corresponding mechanism is included below the chemical reaction:

Global reaction involving water molecules (Fig. 4a):

$$Ag^+ + 2H_2O \rightarrow \left[Ag\left(H_2O\right)_2\right]^+$$

Reaction mechanism:

1) $Ag^+ + H_2O \rightarrow [Ag(H_2O)]^+$
2) $H_2O + [Ag(H_2O)]^+ \rightarrow \left[Ag\left(H_2O\right)_2\right]^+$

Global reaction involving ammonia molecules (Fig. 5a):

$$Ag^+ + 2NH_3 \rightarrow \left[Ag\left(NH_3\right)_2\right]^+$$

Reaction mechanism:

1) $Ag^+ + NH_3 \rightarrow [Ag(NH_3)]^+$
2) $NH_3 + [Ag(NH_3)]^+ \rightarrow \left[Ag\left(NH_3\right)_2\right]^+$

Let us first focus on the elementary steps of the interaction between a silver cation and an uncharged ligand (water or ammonia), as depicted in Figs. 4a and 5a.

Although these ligands are electrically neutral, the MEP reveals the presence of partially positive and negative zones, so that an interaction can occur between the positively charged silver cation and the negative zone (according to MEP) on each ligand.

Elementary step (1) is explained sufficiently well by MEP: it suggests that any of the lone pairs on the water molecule can react with the silver cation (Fig. 4b) to form an intermediate silver complex, $[Ag(H_2O)]^+$; similarly, the lone pair on ammonia will tend to react with the silver cation (Fig. 5b) to form the respective intermediate silver complex $[Ag(NH_3)]^+$.

However, MEP does not provide a good explanation for the selectivity of the interaction between the intermediate silver complex and the second ligand, because each silver complex bears a net positive charge of +1, and it is difficult to distinguish the atom that is more likely to be attacked by this second ligand in the second elementary step on the basis of the MEP color code. This leads to a rather vague understanding of elementary step (2) (Figs. 4b and 5b) when MEP alone is used to explain why the final silver complex is formed. However, we can use the dual descriptor to clarify this situation.

Water and ammonia molecules show no degeneracy in their frontier molecular orbitals, meaning that $p=q=1$. After applying Eq. 3 to these ligands along with the silver cation, as explained before, 3D maps of the DD were generated and are depicted in Figs. 4c and 5c. DD shows that there are two typical regions on these

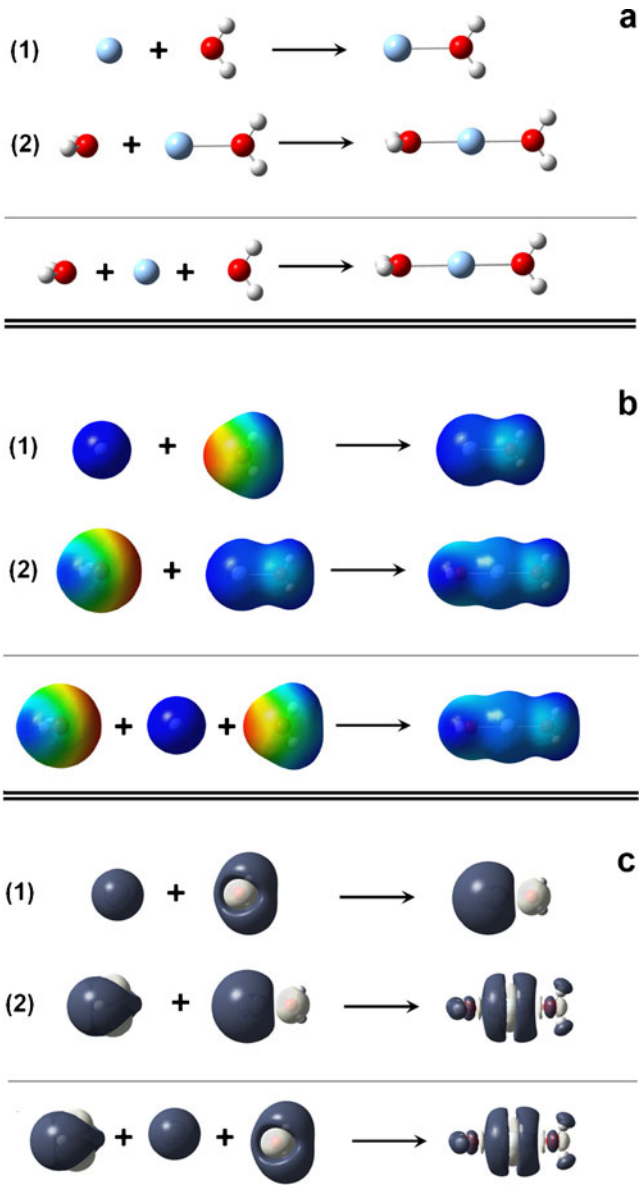

Fig. 4 The reaction mechanism leading to the formation of the silver complex $[Ag(H_2O)_2]^+$. **a** Ball-and-stick model of the reaction mechanism. Atoms are color coded as follows: *red* oxygen, *white* hydrogen, *light blue* silver. **b** The reaction mechanism shown in terms of 3D maps of the molecular electrostatic potential (MEP), $V(\mathbf{r})$. MEP values vary from negative (*red*) to positive (*blue*); *red-colored zones* indicate sites where the effects of electrons are dominant (electrically negative), *green-colored zones* indicate sites where the effects of nuclei and electrons are balanced, while *blue-colored zones* show sites where the effects of nuclei are dominant (electrically positive). The interval $\{V(\mathbf{r})\}_{min} \leq V(\mathbf{r}) \leq \{V(\mathbf{r})\}_{max}$ is therefore depicted. **c** The reaction mechanism shown in terms of 3D maps of the dual descriptor (DD), $f^{(2)}(\mathbf{r})$. A *dark-colored lobe* implies that $f^{(2)}(\mathbf{r})>0$, thus indicating that nucleophilic attacks will preferentially occur there; a *light-colored lobe* implies that $f^{(2)}(\mathbf{r})<0$, thus indicating that electrophilic attacks will preferentially occur there. Isosurfaces of 0.001 a.u. are depicted

ligands, which are depicted by light-colored lobes and dark-colored lobes in the figure.

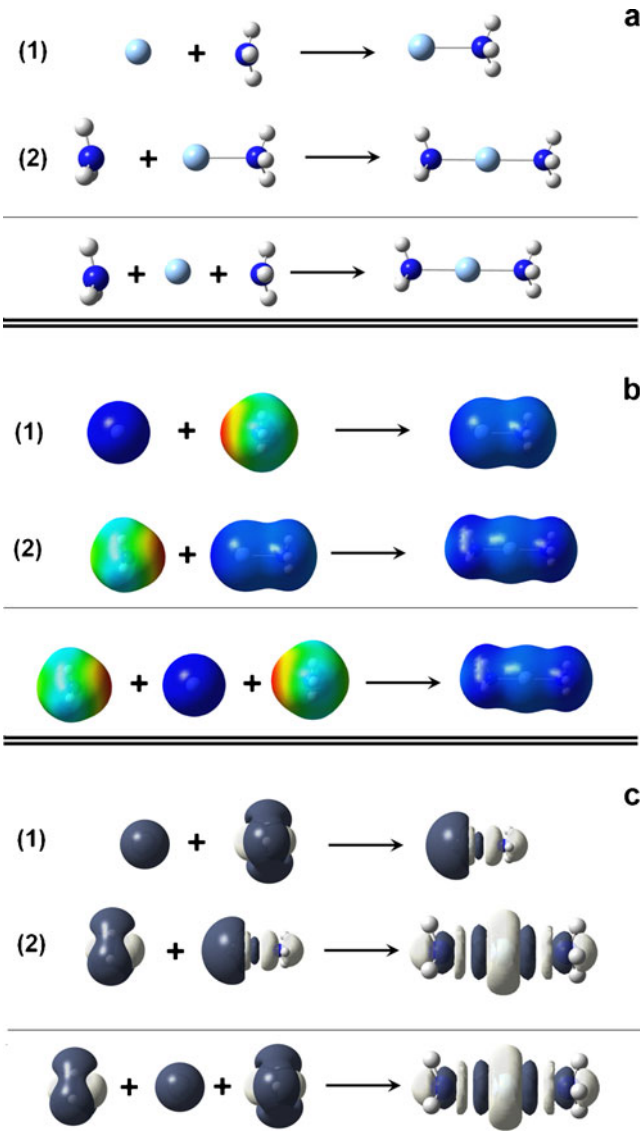

Fig. 5 The reaction mechanism leading to the formation of the silver complex $[Ag(NH_3)_2]^+$. **a** Ball-and-stick model of the reaction mechanism. Atoms are color coded as follows: *blue* nitrogen, *white* hydrogen, *light blue* silver. **b** The reaction mechanism shown in terms of 3D maps of the molecular electrostatic potential (MEP), $V(\mathbf{r})$. MEP values vary from negative (*red*) to positive (*blue*); *red-colored zones* indicate sites where the effects of electrons are dominant (electrically negative), *green-colored zones* indicate sites where the effects of nuclei and electrons are balanced, while *blue-colored zones* show sites where the effects of nuclei are dominant (electrically positive). The interval $\{V(\mathbf{r})\}_{min} \leq V(\mathbf{r}) \leq \{V(\mathbf{r})\}_{max}$ is therefore depicted. **c** The reaction mechanism shown in terms of 3D maps of the dual descriptor (DD), $f^{(2)}(\mathbf{r})$. A *dark-colored lobe* implies that $f^{(2)}(\mathbf{r})>0$, thus indicating that nucleophilic attacks will preferentially occur there; a *light-colored lobe* implies that $f^{(2)}(\mathbf{r})<0$, thus indicating that electrophilic attacks will preferentially occur there. Isosurfaces of 0.001 a.u. are depicted

Elementary step (1) is then understood as the consequence of the favorable covalent interaction (Figs. 4c and 5c) caused by the overlap of the light-colored lobe of the first ligand with the dark-colored lobe of the silver cation, yielding the first intermediate silver

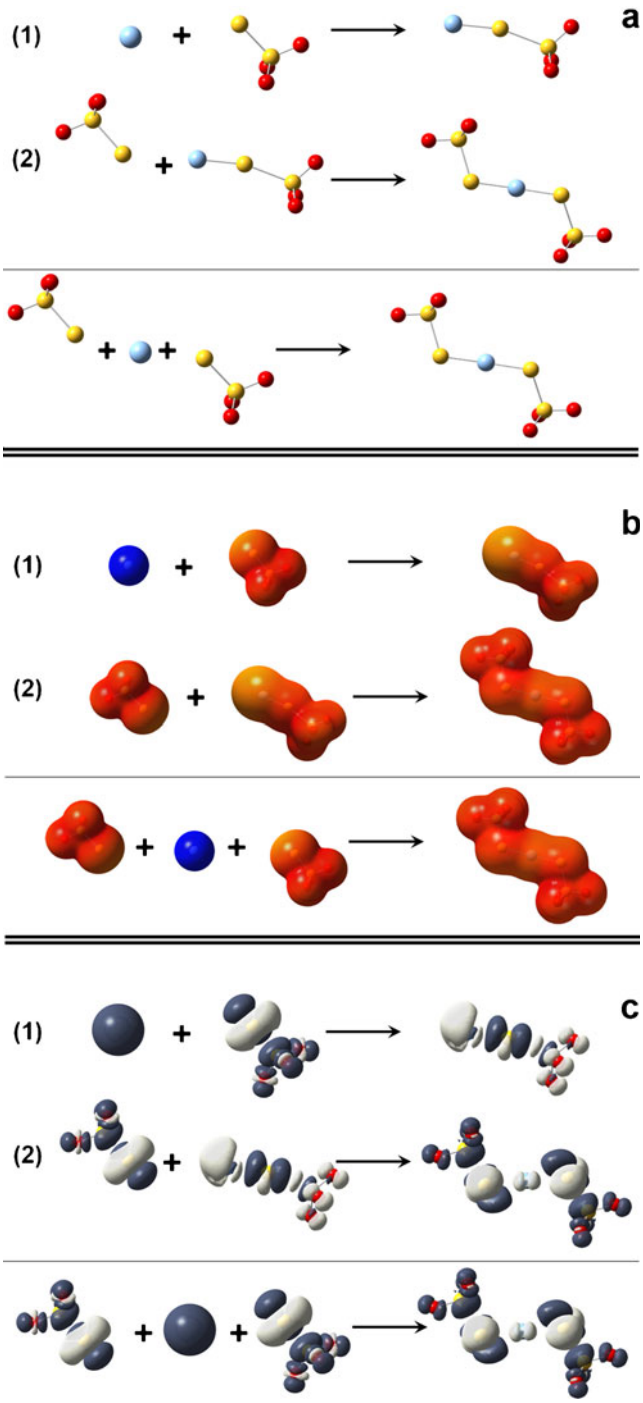

Fig. 6 The reaction mechanism leading to the formation of the silver complex $[Ag(S_2O_3)_2]^{3-}$. **a** Ball-and-stick model of the reaction mechanism. Atoms are color coded as follows: *red* oxygen, *yellow* sulfur, *light blue* silver. **b** The reaction mechanism shown in terms of 3D maps of the molecular electrostatic potential (MEP), $V(\mathbf{r})$. MEP values vary from negative (*red*) to positive (*blue*); *red-colored zones* indicate sites where the effects of electrons are dominant (electrically negative), *green-colored zones* indicate sites where the effects of nuclei and electrons are balanced, while *blue-colored zones* show sites where the effects of nuclei are dominant (electrically positive). The interval $\{V(\mathbf{r})\}_{min} \leq V(\mathbf{r}) \leq \{V(\mathbf{r})\}_{max}$ is therefore depicted. **c** The reaction mechanism shown in terms of 3D maps of the dual descriptor (DD), $f^{(2)}(\mathbf{r})$. A *dark-colored lobe* implies that $f^{(2)}(\mathbf{r})>0$, thus indicating that nucleophilic attacks will preferentially occur there; a *light-colored lobe* implies that $f^{(2)}(\mathbf{r})<0$, thus indicating that electrophilic attacks will preferentially occur there. Isosurfaces of 0.001 a.u. are depicted

complex (the DD of which also presents these typical regions). In turn, elementary step (2) can be explained again as favorable overlap of the dark-colored lobe of the intermediate complex with the light-colored lobe of the second ligand [water or ammonia in step (2) in Figs. 4c and 5c, respectively], which produces the final silver complex. Note that the maximum overlap between the lobes of DD was used as a qualitative criterion to explain the selectivity observed in these reactions.

Thus, the DD indicates that the silver atom of the first intermediate complex, which acts as a electrophile, will be attacked by the nucleophilic atom of the ligand: oxygen in the water molecule or nitrogen in the ammonia molecule. This information cannot be deduced through the sole use of the MEP; nevertheless, it is important to state that the MEP is able to predict the final silver complex when it is applied to the global reaction, not to each elementary step (see the global reactions in Figs. 4b and 5b). This is because, in the global reaction, the negative MEP zones of the ligand are able to interact favorably with the silver cation.

To sum up, the long-range interactions between the silver cation and the ligands are mainly electrostatic in nature, but covalent interactions become more important at short interaction distances because the selectivity is correctly described using the dual descriptor. Thus, MEP and DD complement each other as tools for understanding these reaction mechanisms: MEP explains the long-range interactions while DD describes the short-range interactions (when they cannot be explained using solely MEP). The first elementary step in this type of mechanism is mainly controlled by electric charges (i.e., it is charge-controlled), although favorable covalent interactions are also present (as supported by DD). Meanwhile, the second elementary step is totally frontier-controlled, as these orbitals determine the selectivity, so this step cannot be interpreted using MEP.

The reaction between a silver cation and a thiosulfate anion can also be analyzed in terms of the MEP and the DD. The global reaction involving thiosulfate molecules (Fig. 6a) is as follows:

$$Ag^{+} + 2S_2O_3^{2-} \rightarrow \left[Ag\left(S_2O_3\right)_2\right]^{3-}$$

The reaction mechanism can be split into two elementary steps:

1) $Ag^+ + S_2O_3^{2-} \rightarrow [Ag(S_2O_3)]^-$
2) $S_2O_3^{2-} + [Ag(S_2O_3)]^- \rightarrow [Ag(S_2O_3)_2]^{3-}$

In this case, the global electrostatic interaction between the silver cation and the first thiosulfate anion can be accurately interpreted by using MEP to analyze the reaction mechanism (Fig. 6b), but the interactions that occur between specific atoms in both elementary steps cannot be understood by applying this local reactivity descriptor.

Moreover, the partially negative MEP zone in thiosulfate is where the oxygen atoms are concentrated, but the terminal sulfur is the atom that preferentially reacts with the silver cation in elementary step (1), as depicted in Fig. 6b. Although the silver cation is attracted to the thiosulfate anion due to a long-range electrostatic interaction between them, the short-range interaction between these two species is ruled only by the frontier molecular orbitals (see the first elementary step in Fig. 6c), thus leading to the first intermediate silver complex, which reacts with the second thiosulfate anion to produce the final silver complex, as expected, during elementary step (2). Note that, for all of the thiosulfate anions in Fig. 6c, the DD exhibits dark-colored and light-colored lobes that are localized around the terminal sulfur atom, and the light-colored one is the lobe that predominantly interacts with the silver cation. The oxygen atoms of thiosulfate cannot interact favorably with the silver cation, so chemical bonds are formed between the terminal sulfur atoms and the silver cation.

Conclusions

This work has shown that the dual descriptor is a useful tool that complements the molecular electrostatic potential, which accurately predicts long-range ionic interactions between two species; for instance, the interaction of a silver cation (Ag^+) with a charged or uncharged ligand molecule $L = \{CN^-; S_2O_3^{2-}; H_2O; NH_3\}$. In almost all of the reactions presented here, the first elementary step was well explained by the MEP—even when L was a uncharged molecule, because the interaction involved was charge-controlled (at least at long interaction distances). However, an exception was observed when $L = \{S_2O_3^{2-}\}$, as detailed below.

MEP indicated that the first elementary step is totally charge-controlled (at long and short interaction distances) when $L = \{H_2O; NH_3\}$ (i.e., ligands with a net charge of zero), because Ag^+ interacts with the partial negative charge of L, thus yielding the first cationic silver complex, AgL^+. On the other hand, when $L = \{CN^-; S_2O_3^{2-}\}$ (which have net charges of −1 and −2, respectively), the first elementary step is only partially charge-controlled (i.e., only at long interaction distances)—although the MEP indicates that a favorable long-range electrostatic interaction occurs between the silver cation and the respective anion, MEP cannot indicate which of the atoms in the ligand will tend to participate in a short-range interaction with the silver cation. Thus, it is necessary to apply a local reactivity descriptor that can highlight which atom in the ligand will tend to form a bond with the silver cation. This descriptor is known as the dual descriptor.

The second elementary step can be understood as a charge-controlled, long-range reaction between the first silver complex AgL and a second ligand L, leading to the formation of the final complex AgL_2. At short interaction distances, the reaction is frontier-controlled. An exception occurs when $L = \{S_2O_3^{2-}\}$, because in this case the first intermediate silver complex, $[Ag(S_2O_3)]^-$, is negatively charged, and thus repels the second $S_2O_3^{2-}$ ligand. Therefore, when $S_2O_3^{2-}$ (or indeed any other negatively charged ligand with a greater absolute charge than the charge on the cation) is involved, the respective elementary step is totally frontier-controlled (at both long and short interaction distances). As a consequence, an LRD such as the DD must be applied to accurately interpret the favorable interaction between two negative species, because the DD can identify the covalent interactions that are involved in the reaction.

The analysis performed in the present work demonstrated that the dual descriptor is very simple to use, but at the same time it is a powerful tool for understanding reaction mechanisms that cannot be explained by the MEP alone. Therefore, based on this work, the DD can be considered a useful complementary tool to the MEP that must be taken into account when covalent interactions dominate over ionic interactions.

Acknowledgments This work was partially financed by funding from the Vice-Rector of Research and Development to promote and support research in the UPV university community, so the author wishes to thank the financial support afforded by Fondo VRID no. 000012A26 (Fondo Vicerrectoría de Investigación y Desarrollo) from UPV and FONDECYT grant no. 11100070 (A Project for Research Initiation), which provided computational equipment and software.

References

1. Politzer P, Murray JS (2002) Theor Chem Acc 108:134–142
2. Murray JS, Politzer P (2011) The electrostatic potential: an overview. WIREs Comput Mol Sci 1:153–163
3. Hohenberg P, Kohn W (1964) Phys Rev B 136:864–871
4. Kohn W, Sham LJ (1965) Phys Rev A 140:1133–1138
5. Geerlings P, De Proft F, Langenaeker W (2003) Chem Rev 103:1793–1873
6. Chermette H (1999) J Comput Chem 20:129–154

7. Morell C, Grand A, Toro-Labbé A (2005) J Phys Chem A 109:205–212
8. Morell C, Grand A, Toro-Labbé A (2006) Chem Phys Lett 425:342–346
9. Toro-Labbé A (2007) Theoretical aspects of chemical reactivity, vol 19. Elsevier, Amsterdam
10. Ayers PW, Morell C, De Proft F, Geerlings P (2007) Chem Eur J 13:8240–8247
11. Morell C, Ayers PW, Grand A, Gutiérrez-Oliva S, Toro-Labbé A (2008) Phys Chem Chem Phys 10:7239–7246
12. Morell C, Hocquet A, Grand A, Jamart-Grégoire B (2008) THEOCHEM 849:46–51
13. Cárdenas C, Rabi N, Ayers PW, Morell C, Jaramillo P, Fuentealba P (2009) J Phys Chem A 113:8660–8667
14. Fuentealba P, Parr RG (1991) J Chem Phys 94:5559–5564
15. Parr RG, Yang W (1989) Density-functional theory of atoms and molecules. Oxford University Press, New York, pp 95–97
16. Flores-Moreno R (2010) J Chem Theory Comput 6:48–54
17. Martínez J (2009) Chem Phys Lett 478:310–322
18. Martínez JI, Moncada JL, Larenas JM (2010) J Mol Model 16:1825–1832
19. Schlegel HB (1982) J Comput Chem 3:214–218
20. Becke AD (1988) Phys Rev A 38:3098–3100
21. Becke AD (1993) J Chem Phys 98:5648–5652
22. Becke AD (1993) J Chem Phys 98:1372–1377
23. Lee CL, Yang W, Parr RG (1988) Phys Rev B 37:785–789
24. Jeffrey Hay P, Wadt WR (1985) J Chem Phys 82:270–283
25. Jeffrey Hay P, Wadt WR (1985) J Chem Phys 82:299–310
26. Frisch MJ et al (2010) Gaussian 09, revision B.1. Gaussian, Inc., Wallingford
27. Pearson RG (1963) J Am Chem Soc 85:3533–3543
28. Pearson RG, Songstad J (1967) J Am Chem Soc 89:1827–1836
29. Pearson RG (1968) J Chem Educ 45:581–587
30. Pearson RG (1987) J Chem Educ 64:561–567
31. Gázquez JL (1997) J Phys Chem A 26:4657–4659